International Journal of Biological Macromolecules 220 (2022) 1444–1453

Contents lists available at ScienceDirect

International Journal of Biological Macromolecules

journal homepage: www.elsevier.com/locate/ijbiomac

Surface chemistry and bioactivity of colloidal particles from industrial kraft lignins

Oihana Gordobil [a,*], Huisi Li [b], Ana Ayerdi Izquierdo [c], Ainhoa Egizabal [c], Olena Sevastyanova [b,d,*], Anna Sandak [a,e]

[a] InnoRenew CoE, Livade 6, 6310 Izola, Slovenia
[b] Department of Fiber and Polymer Technology, School of Chemistry, Biotechnology and Health, KTH Royal Institute of Technology, Teknikringen 56-58, Stockholm 100 44, Sweden
[c] TECNALIA, Basque Research and Technology Alliance (BRTA), Mikeletegi Pasealekua 2, Donostia-San Sebastian 20009, Spain
[d] Wallenberg Wood Science Center, WWSC, School of Chemistry, Biotechnology and Health, KTH Royal Institute of Technology, Teknikringen 56-58, Stockholm 100 44, Sweden
[e] University of Primorska, Faculty of Mathematics, Natural Sciences and Information Technologies, Glagoljaska 8, 6000 Koper, Slovenia

ARTICLE INFO

Keywords:
Kraft lignin
Colloidal particles
Morphology
Surface chemistry
Antioxidant activity
Cytotoxicity

ABSTRACT

The morphology control of lignin through particle size reduction to nanoscale seems to be a suitable conversion technology to overcome the intrinsic limitations of its native form to develop a wide range of biomaterials with high performance. Colloidal lignin particles (CLPs) in the range of 150–200 nm were synthesised from hardwood and softwood kraft lignins by the solvent shifting method. The initial molecular features of kraft lignins were evaluated in terms of purity, molecular weight distribution, and chemical functionalities. The impact of the lignin source and structure on the morphology, size distribution, and surface chemistry of CLPs was evaluated by particle size analyser, SEM, TEM and ^{1}H NMR. The results evidenced the influence of the botanical origin on the morphology and surface chemistry of particles. Furthermore, the antioxidant properties and cytotoxicity of lignins and corresponding CLPs, towards lung fibroblast cells were compared. CLPs from hardwood kraft lignins exhibited higher antioxidant power against DPPH free radical and a higher cytotoxic effect (IC_{30} = 67–70 μg/mL) against lung fibroblast when compared to CLPs from softwood kraft lignin (IC_{30} = ~91 μg/mL). However, the cytotoxicity of these biomaterials was dose-dependent, suggesting their potential application as active ingredients in cosmetic and pharmaceutic products at low concentrations.

1. Introduction

The growing interest in lignin polymer in the recent years lies in its unique versatility and abundance both in nature and at the industrial level. In the last two decades kraft lignin, a by-product from the pulp and paper industry which is generated in large quantities annually worldwide (approximately 50 million tons), has revealed an enormous potential for valorisation into a wide range of chemicals and biomaterials [1]. However, lignin in its original state presents some technical limitations such as high heterogeneity, dark colour, low solubility in water and poor compatibility with polymers, therefore, it usually needs a conversion process to provide high-performance when is used in specific applications.

In the recent years, lignin-based nanomaterials such as nanoparticles, nanotubes, and nanofibres have received a great deal of attention because of their extraordinary characteristics and functionalities which offer additional advantages for lignin valorisation in the field of materials and healthcare [2]. Morphology control through particle size reduction to the nanoscale seems to be one of the most suitable strategies to overcome the limitations of irregular lignin powder for the development of lignin-based products with high-performance.

Spherical lignin nanoparticles (LNPs) have been produced by different approaches and a combination of chemical and physical methods [3,4]. Solvent sifting method is one of the most explored to produce nanosized particles from lignin. The process consist of dissolving lignin in a water miscible organic solvent and precipitating in a non-solvent (typically water), where lignin is not soluble and tends to assembly into spherical-like shape particles (solid or hollow) [5,6]. The

* Corresponding authors.
E-mail addresses: oihana.gordobil@innorenew.eu (O. Gordobil), olena@kth.se (O. Sevastyanova).

https://doi.org/10.1016/j.ijbiomac.2022.09.111
Received 1 August 2022; Received in revised form 8 September 2022; Accepted 12 September 2022
Available online 16 September 2022
0141-8130/© 2022 Published by Elsevier B.V.

major disadvantage of this process is the low concentration of particles in the colloidal suspension.

Nowadays, the production of homogeneous and nanoparticles from lignin polymer aimed at partially or totally substituting the fossil components in a wide variety of products and formulations, such as composites [7], coatings [8], and sunscreens [9] to obtain new or desirable properties of the base products providing antimicrobial and antioxidant properties, thermal resistance, and UV filtering ability. Moreover, lignin nanoparticles have been used for the stabilisation of immiscible liquids by the formation of Pickering emulsions, opening new opportunities for their use in the food, cosmetic, and biomedical sectors where non-toxic emulsifiers are desired [10]. There is a focus on the design and development of smart lignin-based carriers for loading active substances through entrapment or encapsulation for drug delivery systems in fertilizers [11], pesticides [12], and biomedicine [13]. Additionally, one of the great advantages of LNPs is the possibility to manipulate their surface characteristics through functionalisation or chemical modification, increasing their range of applications, especially in the field of healthcare, such as the enhancement of cellular interactions with specific cells for medical diagnostic or therapeutic applications [13–17] as well as stabilisation against extreme pH or solvent conditions [18].

Therefore, considering the increasing trend of the cosmetic, pharmaceutical, and biomedical sectors that demand bio-based alternatives, lignin nanoparticles represent a revolutionary opportunity in healthcare applications. However, compounds from renewable sources like lignin cannot be classified as safe or biocompatible based on their natural origin, and therefore, cytotoxic analyses are essential, not only to ensure the biocompatibility of this aromatic compound, but also to provide further insight into the biological profile of the lignin polymer at nanoscale, since the toxicological aspects related to nanomaterials is usually a topic of great concern [19]. Although numerous advances have been made in the field of lignin-based nanomaterials, lignin complexity and the lack of fundamental comprehension of the behavior of this natural polymer at nanoscale makes it difficult to understand the relationship between the structure-properties-performance of nanoparticles.

In this research, colloidal lignin particles (CLPs) from hardwood and softwood kraft lignins were synthesised by wet methodology. The molecular structure of lignins was analysed in terms of molecular weight and functional groups, to study the influence of the lignin source on the morphology and size distribution, and surface chemistry of colloidal particles. Furthermore, this research includes the comparison of the antioxidant properties and *in vitro* cytotoxicity towards lung fibroblasts of irregular powder lignins with their corresponding nanoparticles, in order to demonstrate if they are biocompatible with human cells and if they can be safely applied to human skin.

2. Experimental procedure

2.1. Materials

For this study, 3 lignins from kraft pulping operations were selected. Softwood kraft lignin (SKL) was obtained from the Lignoboost process, while hardwood kraft lignins, differing by drying temperature (HKL25 and HKL50), were isolated in a laboratory by acid precipitation, with sulfuric acid, of industrial black liquor as previously described [20]. Klason lignin, acid-soluble lignin (ASL), and ash content were determined to evaluate the purity of industrial lignins. Other solvents and reagents for lignin characterisation including acetone (99.5 %), methanol (99.8 %), dimethyl sulphoxide (99.9 %), D_2O, Folin-Ciocalteau reagent, sodium carbonate (99.5 %), 2,2-Diphenyl-1-picrylhydrazyl, and ascorbic acid were purchased from Sigma Aldrich, Fisher, and Honeywell.

2.2. Methods

2.2.1. Colloidal lignin particles production by wet methodology

The colloidal lignin particles (CLPs) were prepared by the nanoprecipitation method. Lignin samples (1 mg/mL) were dissolved in acetone/water (9:1, *v*/v). The solution was stirred (300 rpm) for 30 min at room temperature and filtered with a 0.22 μm syringe filter to remove undissolved material and impurities. Then, 3 volumes of cold distilled water (10 °C) were added drop by drop to the lignin solution under the effect of ultrasonic treatment (37 kHz) (Elmasonic S) to promote the formation of homogeneous and smaller sized particles. The acetone was evaporated using a rotavapor and the suspension was centrifuged at 6000 rpm for 10 min. The supernatant was used for further analysis.

2.3. Analysis

2.3.1. Characterisation of technical lignins

2.3.1.1. SEC. Molecular weight of lignin samples were determined by size-exclusion chromatography (SEC) according to the protocol reported by Tagami et al. [21].

2.3.1.2. FT-IR. Infrared spectral measurements of crude lignins were performed in an Alpha II compact FT-IR spectrophotometer (Bruker Optik GmbH, Germany) equipped with a diamond crystal. IR spectrum of investigated samples was recorded on attenuated total reflectance mode from an average of 64 scans in the range 4000–400 cm^{-1} at a spectral resolution of 4 cm^{-1}. Three measurements were performed on each lignin sample. Band assignments were based on literature [22,23].

2.3.1.3. ^{31}P NMR. Phosphorous Nuclear Magnetic Resonance (^{31}PNMR) was used for the quantification of functional groups according to Granata and Argyropolous, 1995 [24]. 30 mg of lignin samples (previously dried) were weighed and dissolved in100 μL DMF and 100 μL pyridine under rotation for 30 min at 50 °C until complete dissolution. 50 μL of Endo-N-Hydroxy-5-norbornene-2,3-dicarboximide (e-HNDI) at a concentration of 60 mg/mL in pyridine was added as an internal standard and chromium (III) acetylacetonate (5 mg/mL) was used as a relaxation reagent. Then, 100 μL of phosphorous-containing reagent (2-chloro-4,4,5,5-tetramethyl-1,3,2-dioxaphospholane) was used as a derivatization agent and the derivatized sample was dissolved in 450 μL $CDCl_3$ prior to analysis. The NMR experiment was performed with a 90° pulse angle, inverse gated proton decoupling, and a delay of 10 s. For analysis, 256 scans with a delay of 5 s were collected for a total runtime of 29 min.

2.3.1.4. Thermal analysis. Thermogravimetric analyses were performed using a thermogravimetric analyser Discovery TGA-5500 (Waters TA Instruments, USA). A high-resolution dynamic method at a heating rate of 20 °C/min, final temperature of 800 °C, resolution of 4, and sensitivity value of 1, was used for all samples. For the thermal analysis of lignin fractions, 5–10 mg of lignin was tested under a nitrogen atmosphere from 25 to 800 °C. Then, the samples were maintained under oxygen atmosphere at 800 °C for 15 min to determine the ash content. Three replicates were run for each lignin sample. The electro-balance was purged with nitrogen at a flow rate of 10 mL/min and the furnace at a flow rate of 25 mL/min. Thermogravimetric (TG) and derivative thermogravimetric (DTG) data generated by the instruments were decoded using TA Instruments TRIOS software. DSC analyses were carried out using a dynamic calorimetry system Discovery DSC-25 (Waters TA Instruments, USA). About 5–10 mg of lignin samples were sealed in hermetic aluminium pans and tested under nitrogen atmosphere at a heating rate of 10 °C/min. Samples were first jumped to 105 °C to eliminate interferences due to moisture and to erase the thermal history. Then the samples were cooled to 25 °C and reheated to

200 °C, for determining glass transition temperature (T_g).

2.3.2. Characterisation of colloidal lignin particles

2.3.2.1. Dynamic Light Scattering (DLS). A Zetasizer Nano ZS instrument (Malvern-Pananalytical, Malvern, UK) was used for analysis of the zeta potential, average size, and size distribution of the elaborated lignin particles. All measurements were performed in at least triplicates, 15 s of equilibrium time, and 30 runs of analysis for each repetition at 25 °C. The measurements were performed at 173° in the backscattering mode.

2.3.2.2. SEM and TEM. The morphology of elaborated CLPs was examined under scanning electron microscope (SEM) and transmission electron microscope (TEM). An S-4800 microscope was used (S-4800 Hitachi, Japan) to investigate the morphology of the lignin particles. Samples were first diluted and then drop-cast on a silicon wafer, dried for at least 30 min, and sputter-coated with a 3–3.2 nm layer of Pt—Pd alloy. For the TEM studies, a Hitachi HT7700 series instrument (Hitachi, Japan) was used with an accelerating voltage of 100.0 kV and an emission current of 8.0 μA. Samples were prepared as follows: 5 μL of an CLPs suspension was drop cast onto a 200-mesh copper grid (Ted Pella Inc., USA; prod No 01800-F) and air dried for at least 30 min.

2.3.2.3. ^1H NMR. The surface chemistry of elaborated CLPs was analysed by *^1H NMR*. NMR experiments of CLPs were carried out according to the methodology developed by Pylypchuk et al., 2020 [25] on a Bruker 400 DMX instrument (Bruker Corporation, Billerica, MA) equipped with a 5 mm Bruker BBI probe (Bruker Corporation, Billerica, MA). Various mL of CLPs suspension were centrifuged using a tabletop centrifuge (Eppendorf, model "mini spin plus") for 15 min at 14,200 rpm to concentrate CLPs in a pellet. The supernatant was removed in a decanted position using a Pasteur pipette, and the CLPs were redispersed in 0.6 mL of D_2O. For each experiment, a user-defined pulse sequence applied presaturation followed by excitation sculpting through two consecutive 3-9-19 Watergate blocks. The Watergate segments used gradient ratios of 40:7 for the respective blocks and a binomial delay time (d19) of 200 μs. Optimal 90° pulse lengths were obtained for each sample by halving the pulse length corresponding to the 180° pulse for which the proton free induction decay (FID) signal was the lowest. A total of 1024 scans with 4004 FID data points were obtained per sample, with an acquisition time of 0.5 s and a relaxation delay time of 5.5 s. The resulting data were first processed in TopSpin (version 1.3, patch level 10, Bruker BioSpin) with 64 k data points using a 0.3 Hz exponential multiplication apodization window, and after Fourier transformation and phase correction, the spectra were transferred to MestreNova (version 14.2.2, Mestrelab Research), where a baseline correction was applied.

2.3.3. DPPH assay

The DPPH scavenging activity was assessed according to the method described by Brand-Williams et al., 1995 [26] with some modifications. Dimethyl sulfoxide (DMSO) was used to dissolve industrially derived lignin samples at different concentrations. Different concentrations of colloidal lignin particles were also prepared by redispersing them in distilled water. Then, an appropriate volume of prepared dilution/dispersions were added to DPPH (25 mg/L in methanol) and the absorbance was measured at 517 nm after 30 min of incubation in the dark at room temperature (Mettler Toledo UV7). Ascorbic acid in DMSO was used as a positive control. Each test was carried out in triplicate. The inhibition percentage of the DPPH radical was calculated according to Eq. (1):

$$Inhibition\ (\%) = \frac{Abs_S - Abs_B}{Abs_B} \times 100 \quad (1)$$

where the Abs_S is the absorbance of DPPH at 517 nm in the presence of lignin sample and Abs_B is the absorbance of DPPH at 517 nm containing DMSO in the case of raw lignins and distilled water in the case of CLPs. The radical scavenging activity of the lignin was expressed using the term "efficient concentration" or IC_{50}, which is the concentration required for 50 % inhibition of the free radical.

2.3.4. Cell culture and methyl thiazolyl tetrazolium (MTT) assay

Human lung MRC-5 (ATCC CCL-171) cells were purchased from American Type Culture Collection (LGC Standards) and cultivated following their indications. MRC-5 were suspended in Eagle's MEM (EMEM; Sigma Aldrich) supplemented with 10 % (*v*/v) foetal bovine serum and antibiotics (100 units/mL penicillin, and 100 μg/mL streptomycin), and incubated at 37 °C under a humidified atmosphere with 5 % CO_2 and 95 % air. When cells proliferated in the culture flask to confluence, cells were trypsinised and subcultured. For the assay described in this report, MRC-5 cells were used at 10,000 cells/well into 96-well plate. Cells were incubated for at least 24 h before treatment to allow cell adhesion. Then, the culture medium was removed, and cells were treated with 100 μL of prepared lignin solutions and CLPs dispersions. For raw lignins, 20 mg of sample were dissolved in 1 mL of dimethyl sulfoxide (DMSO). To obtain lignin solutions at different concentrations, serial dilutions using a dilution factor of 2 were performed. Then, 5 μL of each solution were transferred to 995 μL of culture medium. For CLPs, 400 μL of CLPs suspension were mixed with 600 μL of water. Then, serial dilutions using a dilution factor of 2 was also carried out. The methyl thiazolyl tetrazolium (MTT) assay was carried out according to the international standard ISO 10993-5 (ISO 10993 Biological evaluation of medical devices. Part 5: Tests for *in vitro* cytotoxicity) to evaluate the *in vitro* cytotoxicity of raw lignins and CLPs in MRC-5 cells. After 24 h of treatment, the supernatant was removed. After that, the cells were rinsed with phosphate-buffered saline (PBS) (pH = 7.4) and treated with MTT solution (100 μL, 1 mg/mL) at 37 °C and 5 % CO_2 to allow MTT metabolisation for 4 h. Then, the MTT solution was removed and 100 mL of DMSO was added into each well to solubilize formazan (metabolic product of MTT). The number of surviving cells correlates to the colour intensity which is determined by photometric measurements at 570 nm of each well is measured using a microplate reader (Synergy H1 microplate reader, Biotek). For the data analysis, a calculation of cell viability is made for each concentration of the test sample by using the mean of the replicate values per test concentration. This value is compared with the mean of all blank values. Relative cell viability is then expressed as a percentage of untreated blank. ISO 10993-5 states that if the relative cell viability is higher than 70 % of the control group, the material shall be considered non-cytotoxic. Cells treated with DMSO and water were used as a negative control. After a 24 h treatment, each plate was examined under a phase contrast microscope (TS100, Nikon) to identify the morphology of control and treated cells.

2.3.5. Statistical analysis

The means and standard deviations of all the experimental data of the three independent experiments were calculated using Microsoft Excel software. A value of $p < 0.05$ was considered statistically significant.

3. Results and discussion

3.1. Technical specifications and molecular features of raw lignins

Lignin chemistry is mostly related to the origin and processing methods; however, properties such us colour, density, and thermal properties, among others have great importance on the final application. The most important technical specifications of the kraft lignins used in this work are presented in Table 1. As expected, softwood lignin from the LignoBoost process presented higher purity than hardwood kraft lignins isolated by acid precipitation in the laboratory. The results were in accordance with previously published studies [27,28]. Additionally, a

Table 1
Technical specifications, molecular weight, and thermal properties of kraft lignins.

Sample	SKL	HKL25	HKL50
Lignin type	G-type	SG-type	SG-type
Colour	Light brown	Light brown	Dark brown
Klason lignin %	89.7 ± 0.3	73.0 ± 2.1	74.5 ± 0.3
Acid-soluble lignin %	3.5 ± 0.1	10.5 ± 0.2	14.0 ± 0.9
Ash %	0.4 ± 0.0	2.3 ± 0.2	0.9 ± 0.1
Density (kg/m^3)	466.4	376.3	714.3
Mn	564.9	393.0	375.1
Mw	6760.3	2258.9	2157.2
IP	12.0	5.8	5.8
T_g (°C)	151.3	133.2	115.0
T_{max} (°C)	363.3	328.5	342.8
Char at 800 °C (%)	36.6	36.4	35.8

high content of acid-soluble lignin was determined in both kraft lignins for eucalyptus. Other authors also observed higher content of acid-soluble lignin for hardwood kraft lignins [27,29]. Sevastyanova et al., 2006 [30] showed that due to thermal degradation, sugars present in hardwood lignins could form furoic-type structures that can re-condense into aromatic compounds and absorb UV light which affects the measurement of the acid-soluble lignin content and contributes to the dark colour of the lignin sample. Fig. 1 shows the physical appearance of kraft lignins from hardwood and softwood sources. Significant colour difference can be observed between both kraft lignins isolated from an industrial black liquor obtained from Eucalyptus chips. Evidently, the drying temperature greatly affected not only the colour but also the density of lignin powder. Regarding the molecular weight properties, SKL showed the highest average molecular weight and polydispersity in comparison to HKL lignins. Kraft lignins from hardwood showed similar elution profile (*Fig. S1 in Supporting information*). Other authors also found higher molecular weight properties and less ash content for kraft lignin obtained from softwood compared to hardwood [23,31]. As was expected, SKL showed higher glass transition temperature than lignins from Eucalyptus, due to its higher molecular weight, condensed substructures, and high content of phenolic hydroxyls, which restricts the mobility of the molecule by strong intermolecular hydrogen bonding interactions [32]. Softwood kraft lignin also presented the highest thermal stability compared to hardwood kraft lignin, which is in agreement with literature [33].

Structural differences between lignin samples were analysed by FTIR and ^{31}P NMR analytical techniques. FT-IR spectra of lignin samples clearly reflected the main differences related to monomeric composition and functional groups in their chemical structure. Fig. 2 shows vibrations of the fingerprint region in the range of 1800–800 cm^{-1} and *Table S1 (Supporting information)* summarizes the band assignment corresponding to the identification of 19 peaks observed in the investigated lignin samples. Signals between 1400 and 1800 cm^{-1} associated to the carbonyl/carboxyl region (#1), aromatic skeletal vibrations (#2 an #3), and C—H deformation in -CH_3 and stretching in aromatic ring vibration (#4 an #5) were common for all lignins. The main structural differences

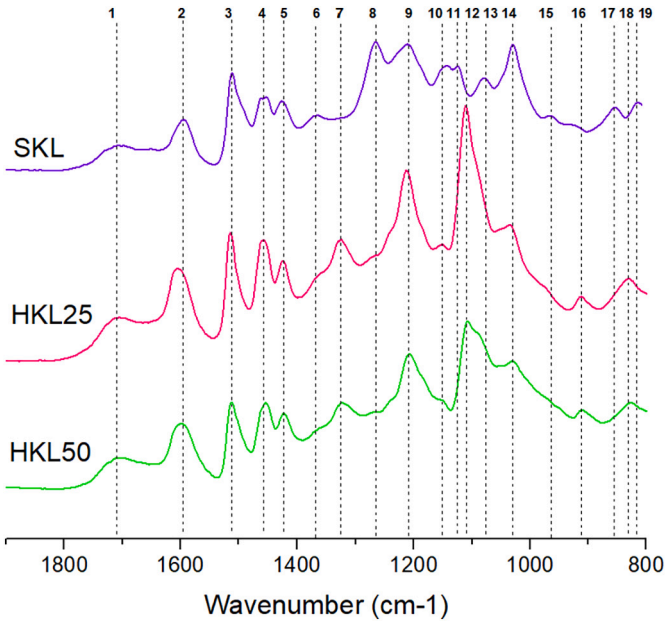

Fig. 2. FT-IR spectra of lignin samples.

were found in the spectral region between 1400 and 900 cm^{-1}, which shows vibrations that are specific to the different elemental units in lignin structure. The weak signal around 1370 cm^{-1} (#6) originating from phenolic -OH and aliphatic C—H in methyl groups appeared as a clear broad band in SKL while in HKL lignins it was barely perceptible. Peak #7 which correspond to 1325 cm^{-1} and is characteristic of syringyl units was only visible in hardwood kraft lignins, while peak #8 (1265 cm^{-1}) associated with guaiacyl units was notably observed only for SKL. The structural differences between samples were also evidenced by the vibration intensities in the spectral region below 1200 cm^{-1}, which is more complex to analyse due to contributions and vibration modes of both lignin and carbohydrates.

The functional groups of lignins were quantified by ^{31}P NMR using the spectral integration limits and assignments previously reported by other authors [34,35]. The amount of aliphatic hydroxyl groups (aliphatic-OH), carboxylic groups (COOH), guaiacyl condensed groups (G-cond-OH), syringyl hydroxyls (S-OH), guaiacyl non-condensed groups (G-non-cond-OH), and *p*-hydroxyphenyl groups (*p*-H-OH) are presented in Table 2. The ^{31}P NMR spectra of the phosphitylated lignin samples are shown in *Fig. S2*. As can be observed, softwood kraft lignin (SKL) presented a higher content of aliphatic hydroxyl groups and more condensed guaiacyl units in its chemical structure than hardwood kraft lignins. However, kraft eucalyptus lignins also presented high content of condensed guaiacyl units and phenolic hydroxyls groups because of the reactions that occurred during kraft pulping. Wei et al. [36] also observed higher G-cond units content in kraft eucalyptus lignin than in lignin that was isolated using mild conditions. Higher content of

Fig. 1. Appearance of kraft lignin samples.

Table 2
Contents of functional groups (mmol/g) determined by ^{31}P NMR.

Functional groups (mmol/g)	Assignments (ppm)	SKL	HKL25	HKL50
Aliphatic-OH	149.0–146.0	2.2	0.8	0.8
5-substituted-OH[a]	144.5-140.5	2.1	3.3	3.6
G-cond-OH[b]	–	2.0	1.4	1.3
S-OH	143.0–142.0	0.1	1.9	2.3
G-non-cond-OH	140.2–138.5	2.1	0.6	0.7
p-H-OH	138.2–137.3	0.2	0.0	0.0
COOH	135.5–134.0	0.5	0.6	0.7
Total Ph-OH	144.0–137.5	4.4	3.9	4.4
Total-OH[c]	–	6.6	4.7	5.1
N/C ratio[d]	–	1.0	2.5	2.3

[a] Sum of S-OH and G-cond−OH.
[b] Area between 144.5 and 140.5 ppm minus area of syringyl phenolic (143–142 ppm).
[c] Sum of aliphatic and phenolic hydroxyl groups.
[d] The ratio of the contents of non-condensed (S-OH + G-non-cond−OH) to condensed (G-cond−OH) phenolic.

carboxylic groups was observed in both HKL. The colour properties of lignin are widely related to its chemical structure. Zhang et al. [37] confirmed that there are some substructures responsible of the dark colour of lignin polymer such as conjugated carbonyl and carboxyl groups, and methoxyls, which have auxochromic effects making the electron transition easier in the lignin chromophores and thus creating a darker colour. According to our results from ^{31}P NMR, the colour difference of lignin samples could be related to the content of S-units and carboxylic groups in their chemical structure.

3.2. Size and morphological properties of CLPs

In this study, water-based colloidal systems from industrial lignins were produced by solvent shifting method using acetone as a recyclable and non-toxic organic solvent. The main drawback of this process was the low concentration and yield of particles in the colloidal system due to the addition of various volumes of water for the precipitation of lignin in the form of nanoparticles. The yield of the CLPs production was <1 % in all cases, 0.76 % for SKL NPs, 0.70 % for HKL25 NPs, and 0.86 % for HKL50 NPs. The concentration of each colloidal system was 0.23 mg/mL for SKL NPs, 0.21 mg/mL for HKL25 NPs, and 0.26 mg/mL for HKL50 NPs.

Average size, polydispersity, and surface charge values of elaborated lignin particles are presented in Table 3. The lowest particle size values were found for particles fabricated from softwood kraft lignin, probably due to its high molecular weight as was previously evidenced by Pylypchuk et al., 2021 [4]. Hardwood kraft lignins, differentiated only by the drying temperature, showed similar particle size average values but different physical properties in terms of surface charge, while particles from HKL dried at 50 °C were more homogeneous than HKL dried at 25 °C. Moreover, the colloidal dispersions showed moderate/good stability according to the zeta-potential results, especially in the case of particles from HKL50. The colloidal particles were eventually measured to assess their stability regarding the size distribution and zeta potential, and the authors did not evidence significant changes during >8 months of evaluation (data not shown).

The morphological characterisation (Fig. 3) was performed by various imaging tests, including TEM and SEM, in order to assess the structure, shape, size, and uniformity of fabricated particles from both softwood and hardwood industrial kraft lignins. Since TEM can help in obtaining information on the inner structures, it revealed that only softwood kraft lignin and hardwood kraft lignin precipitated and dried at 50 °C generated nanoparticles that were solid and spherical in shape. However, we could observe the lesser uniformity in shape of HKL50 NPs compared to SKL NPs, the presence of an external layer with lower density covering the core and particles aggregates, indicating that the raw starting material has a significant effect on the obtained lignin particles. Nanoparticles from hardwood kraft lignin dried at 25 °C (HKL25 NPs), presented a totally different appearance and morphology compared to nanoparticles from HKL50. In the TEM images, non-uniformity and hollow structure of HKL25 NPs can be highlighted. In contrast to other studies where lignin nanoparticles with hollow structure were produced [38], in this work, HKL25 NPs presented quite a thick shell. SEM images allowed for the observation of not only size and shape, but also the surface topology of particles. NPs from SKL showed regular round shape with a smooth surface, while NPs from HKL50 presented a rough surface apparently with a layer covering the nanoparticles. In addition, for HKL25 NPs, SEM images showed the presence of spherical shaped particles with a single and irregular hole in the middle, which is in accordance with the TEM results. Smaller particles presented doughnut-like structures, while larger particles presented a cavity, which in some cases had smaller particles inside. The morphology of this kind of nanoparticle was less regular than the other two studied samples and showed a rough surface as in the case of NPs from HKL50. Results show that morphology control of lignin nanoparticles can be achieved by simply adjusting drying temperatures during lignin recovery.

Table 3
Average size, polydispersity and surface charge of lignin particles.

Sample	Lignin type	Particle size average (nm)	Polydispersity	Zeta potential (mV)
SKL NPs	G	151.2 ± 1.9	0.14	−29.3
HKL25 NPs	SG	185.1 ± 1.5	0.17	−32.5
HKL50 NPs	SG	180.9 ± 0.3	0.09	−51.8

3.3. Surface chemistry of CLPs

In this work, a recently developed method for liquid-state ^{1}H NMR using a combination of presaturation and excitation sculpting water suppression was applied to the analysis of fabricated particles [25]. This new method is suitable for qualitatively evaluating the surface chemistry of the particles from lignin polymer since the use of an aqueous suspension (D_2O) instead of common organic solvents for the analysis keeps intact the original structure of the particles without destroying or deteriorating them. ^{1}H NMR results are presented in the Fig. 4 and the resonances were assigned according to literature [25,39–41]. As can be observed, in contrast to common ^{1}H NMR spectra of lignin, the spectra of CLPs showed only a very weak peak at ~6.8 ppm in the aromatic region (8–6 ppm) which corresponded to protons in aromatic S and G units [41]. The low signal intensity in this region can be related to the low concentration of the sample or to the conformation of the polymer forming the nanoparticle [25]. According to previously reported mechanism for lignin nano-sized particle formation, when dissolved lignin is precipitated in water (antisolvent), it is assembled forming a core-shell structure with a similar behavior to those amphiphilic molecules, where hydrophobic regions, consisting of high Mw aromatic structures are assembled first forming the core of the particle. On the access of water followed by acetone removal, most polar lignin molecules, having a lower Mw and higher content of charged groups, are adsorbed on the surface of particle core, forming a low-density layer. This layer can be observed by TEM and can be detected by ^{1}H NMR [25,42]. For SKL, weak signals were detected at 5.60 ppm and 4.13 ppm, which were attributed to H_α in β-5 of phenylcoumaran structure and H_γ in β-O-4́structure [39,41,43], respectively. Moreover, clear differences were found in the spectral region between 4 and 3 ppm of studied particles. In CLPs from hardwood lignins, signals corresponding to protons of methoxyl groups from S and G units were evidenced at 3.7–3.6 ppm. These signals were significantly less intense in HKL25 compared to HKL50. It can be related to the less total phenolic content (S and G units) of the original chemical structure detected by ^{31}P NMR. In SKL, signals

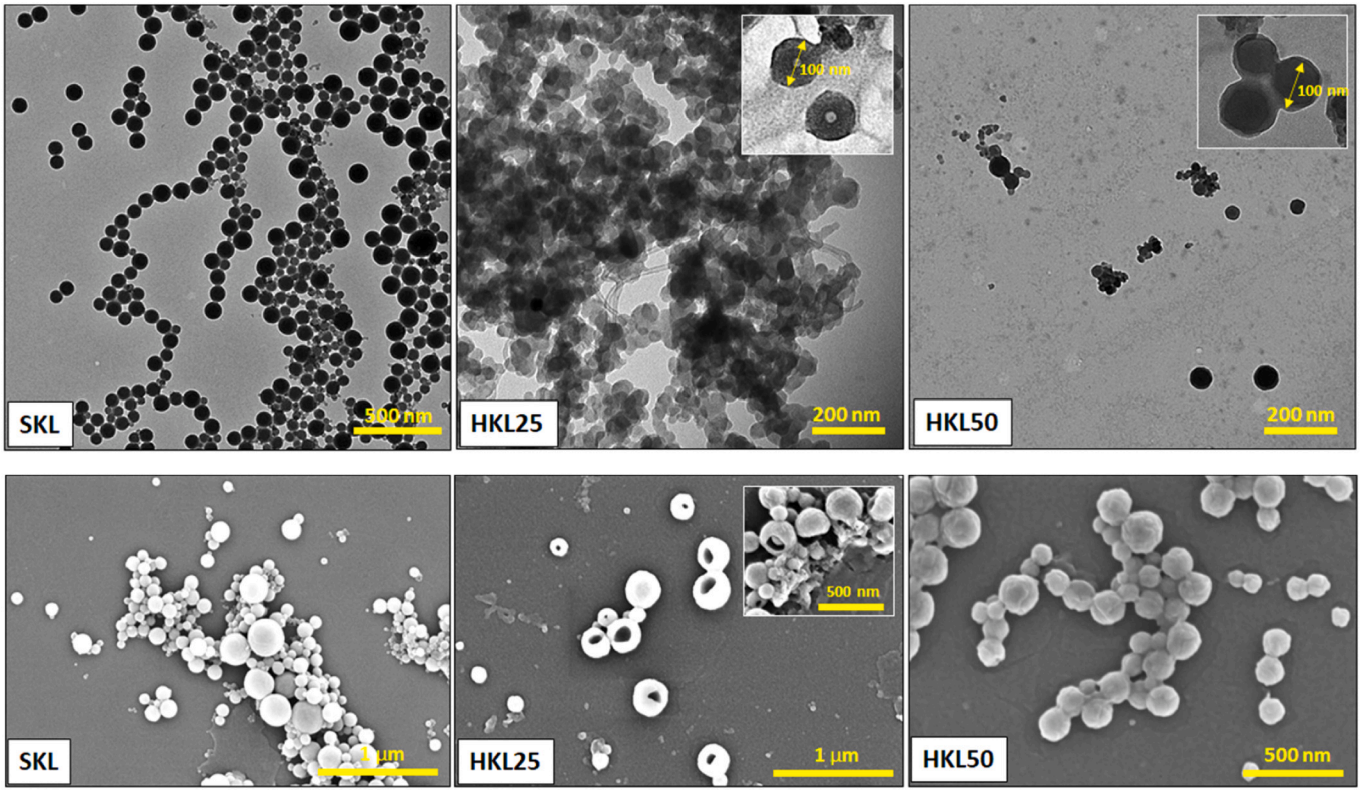

Fig. 3. TEM (top) and SEM (bottom) images of lignin colloidal particles prepared by solvent shifting method from industrially derived lignins SKL, HKL25 and HKL50.

between 3.85 and 3.62 ppm with a sharp peak at 3.73 ppm were attributed to methoxyls in G units. In addition, the presence of H_β in phenylcoumaran and γ-hydroxylated β-O-4′ structures, associated with signals at 3.58–3.36 ppm, were seen only in SKL lignin [25]. The detection of protons related to phenylcoumaran substructure (β-5 linkage) only in the surface of CLPs from softwood kraft lignin can be related to the initial chemical structure where a higher abundance of condensed linkages, such as β-5 due to the free C_5 position of guaiacyl units [44–46], is commonly found. Furthermore, we could observe a sharp peak at 3.26 ppm for HKL NPs, which was less intense for SKL NPs, associated with H_β in β−β′ resinol or protons in xylan substructures. These results are in agreement with literature since xylan is the main hemicellulosic component of hardwoods and is usually found as an impurity related to carbohydrates in hardwood kraft lignins [47]. β−β′ linkages are commonly more abundant in hardwood than softwood lignins [44] and the presence of this kind of substructure in both hardwood NPs was confirmed also by the weak peak detected at 2.66 ppm which was attributed to benzylic protons in β-β′ structures [25,48]. Furthermore, at 2.35 ppm a weak peak related to aromatic acetates was detected only in SKL NPs surface [43]. This is in agreement with a previously published study where this band was only detected in particles from softwood kraft lignin fractions [25]. According to previous works, signals between 0 and 1.6 ppm corresponded to non-oxygenated aliphatic protons of the aliphatic side chain (-CH_2- and -CH_3) and hydrocarbon contaminant [25,41].

3.4. Antioxidant and cytotoxic properties of kraft lignins and CLPs

The capacity of lignin polymer to neutralise the radical species originating from atmospheric oxygen (ROS) as well as to inhibit the oxidation of vegetable oils [49,50], make it a promising natural alternative to synthetic antioxidants in the cosmetic, pharmaceutical, and food processing industries, among others [50–52]. As was previously reported, the radical scavenging activity of lignin is mainly related to the phenolic hydroxyl groups which can form phenoxy radicals stabilising the radical species [53]. However, substituents like methoxyls and other functional groups like conjugated double bonds play a crucial role in stabilising the formed phenoxy radicals favouring extensive electronic delocalisation and in increasing its antioxidant properties [50,54–56]. Nevertheless, lignin is soluble under alkaline conditions and partially soluble in organic solvents in its raw form, which is usually not applicable in skin cosmetics. Therefore, lignin particles dispersed in water seems to be the best strategy to incorporate this natural compound as an ingredient in several products and materials.

The inhibitory effect of industrially derived softwood and hardwood kraft lignins and their corresponding lignin particles were evaluated by DPPH spectrophotometric method, which is considered as an accurate and economic method to assess antiradical activity of natural compounds like plant extracts and lignin polymer. Fig. 5 displays the IC_{50} values of lignin in raw, in nanosized form, and ascorbic acid, a common commercial antioxidant widely used in several fields. Regarding raw lignins, SKL and HKL50 showed similar antioxidant power with IC_{50} values around 12 μg/mL, while HKL25 showed higher IC_{50} value (around 17 μg/mL) probably due to the lower content of phenolic hydroxyls groups in its chemical structure.

Several authors reported that the particle size reduction of lignin results in an improvement of its antioxidant properties [2,5,50,57]. However, in this research, an enhancement in the antioxidant power against DPPH radical (increase of 30 % of the IC_{50} value) was only observed for those particles elaborated from hardwood kraft lignins, while a reduction of 35 % was noticed in particles obtained from softwood. Therefore, there is a clear dependence on the surface chemistry and not simply on the particle size. Bertolo et al. [58] isolated lignin from sugarcane bagasse using alkaline and organosolv processes and prepared nanoparticles by solvent shifting and direct dialysis methods. The antioxidant power tested by DPPH showed that CLPs produced from

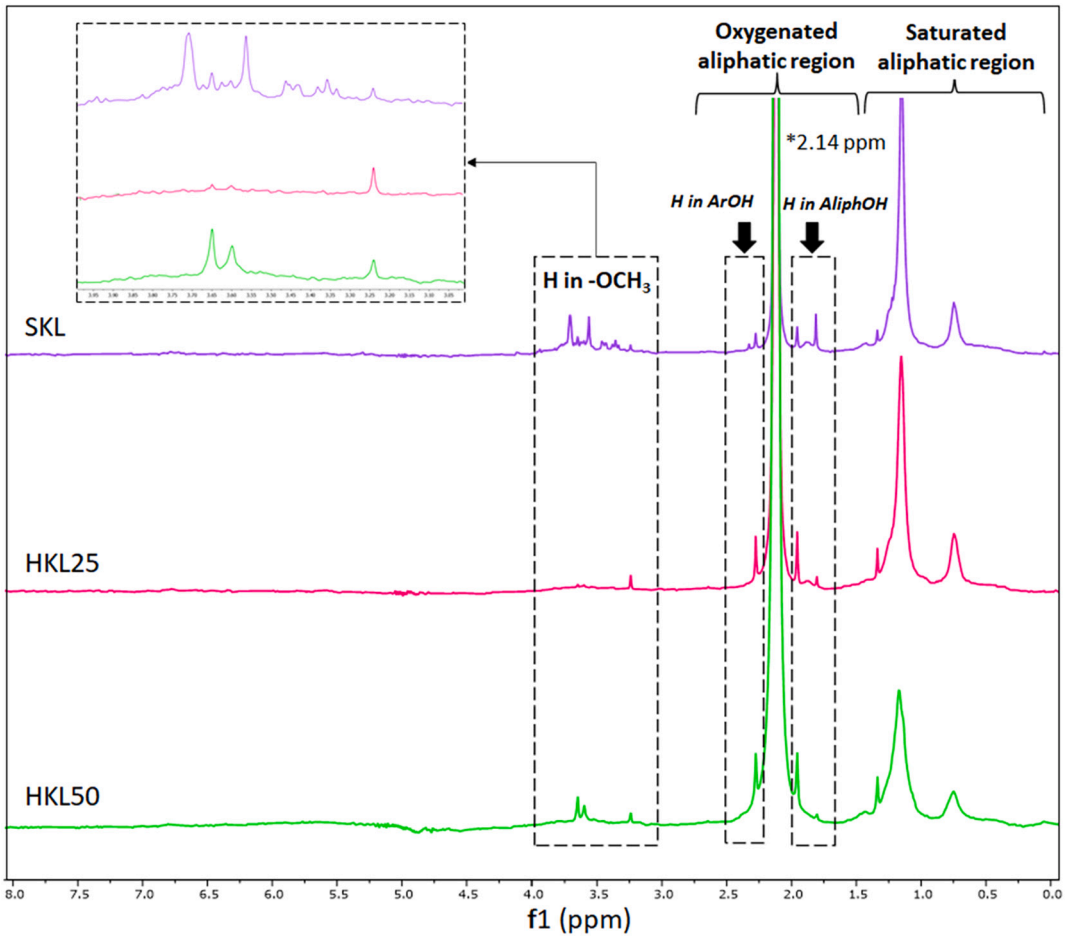

Fig. 4. ^{1}H NMR spectra for lignin NPs from softwood and hardwood kraft lignins (*signal of residual acetone at 2.14 ppm).

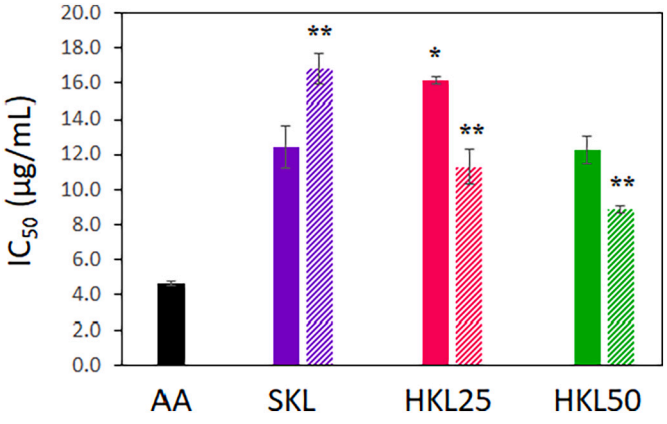

Fig. 5. Efficient concentration value (IC50) from DPPH test. (Solid bar and striped bar correspond to raw lignins and CLPs, respectively). The population means are significantly different at the 0.05 level according to a one-way analysis of variance (ANOVA). *The difference between the means is significant at the 0.05 level when comparing raw lignin samples, according to Bonferroni and Tukey tests. **The difference between the means is significant at the 0.05 level when comparing colloidal lignin particles (CLPs), according to Bonferroni and Tukey tests.

organosolv process, which had less syringyl units in its monomeric composition compared to alkali lignin, was also reduced. Other authors also evidenced slightly lower antioxidant capacity of lignin in the nanoparticle state than in the raw form with lignins from different sources, suggesting that the preparation of nanoparticles does not ensure an improvement in antioxidant properties [59], since it is dependent on the lignin source, isolation treatment, and nanoparticle production method.

Therefore, due to the molecular complexity of lignin polymer, and the lack of knowledge about the relationship of nanostructured lignin-properties, it is difficult to provide an explanation regarding the opposite antioxidant behavior of nanoparticles from softwood and hardwood sources in this work. However, according to literature, kraft lignin contains large amounts of condensed structures that are formed in the final stage of the pulping process, and especially those coming from softwood that consist mostly of guaiacyl-type units with a vacant C_5 position in the aromatic ring [46]. N/C ratio calculated from ^{31}PNMR evidenced the higher degree of condensation of SKL compared to hardwood lignin. Moreover, higher Mw lignins usually contains higher β-O-4 linkages in the chemical structure [60]. In this study, ^{1}HNMR analysis of particles revealed that the main differences in the surface chemistry between nanoparticles of different biological origin was based on the presence of β-5, β-O-4 substructures, and aromatic acetates, which were only detected in SKL NPs. These substructures in the surface of nanoparticles from SKL, associated with condensed structures and etherified/esterified phenolic hydroxyls, could be responsible for the reduced antioxidant power compared to the nanoparticles from hardwood which did not show these substructures on the surface [61].

The literature on nanotoxicology associates the toxic effect of nanosized materials mainly to their shape, surface chemistry, and charge [62]; however, the interaction mechanism of lignin nanoparticles with different culture systems is still not fully understood. In this study, the cytotoxic activity of industrially derived softwood (SKL) and

hardwood kraft lignins (HKL25 and HKL50) and their corresponding CLPs towards lung fibroblast cells at different concentrations (0–100 μg/mL) was evaluated. The solubility of lignin samples in DMSO as well as the resulting concentration of particles in the colloidal suspension from the solvent shifting method limited the evaluation of higher concentrations. The cell viability results and IC_{30} value of raw lignins and their corresponding nanoparticles are summarized in Table 4. After 24 h contact with raw lignin solutions, the cell survival rate at 100 μg/mL of concentration was higher than 85 % for SKL, lower than 60 % for HKL25 and around 20 % for HKL50, indicating that both hardwood kraft lignins showed higher cytotoxic effect than softwood kraft lignin on the studied cells at high concentrations. Other authors suggest that the low molecular weight of lignins contributes to their cytotoxic properties in the powder form [63,64]. In this work, SKL with M_w of 6760.3 g/mol showed no cytotoxic effect compared to both HKL25 and HKL50 with M_w of 2258.9 g/mol and 2157.2 g/mol, respectively.

In addition, when cells were exposed for 24 h to CLPs at the highest concentrations (100 μg/mL), the cell viability was below 70 %, which is considered toxic. However, also in the form of nanoparticles SKL showed lower cytotoxic effect than nanoparticles from hardwood. Lower concentrations of lignin and CLPs did not decrease the cell viability, indicating that the cells were substantially not affected. Previous studies reported that the cytotoxic activity of lignin and lignin particles is exposure-dose and time dependent. Freitas et al., 2020 [65] studied the cytotoxic effect of organosolv lignin micro- and nanoparticles against Caco-2 cells and showed a cellular compatibility of particles after 4 h of contact at high concentrations of 200 μg/mL, while after 24 h of exposure the cell viability was reduced below 70 %. Figueiredo et al. [66] also found an *in vitro* cytocompatibility of the CLPs after incubation for 6 h using different cancer cell lines.

Figs. S3 and S4 presents the effect of lignin samples on the cellular morphology of lung fibroblast cells (MRC-5) treated with dissolved raw lignins and CLPs. The micrographs evidenced morphological features of apoptosis after 24 h in contact with dissolved hardwood lignins but no cellular stress was evidenced at high concentration of SKL. In the case of CLPs the images confirmed that cells vacuolated or collapsed after 24 h of exposure with all synthesised CLPs.

4. Conclusions

Colloidal lignin particles (CLPs) in the range of 150–200 nm were produced from hardwood and softwood kraft lignins by solvent shifting method using a recyclable and non-toxic organic solvent. Concerning the lignin source, softwood kraft lignin (SKL) presented higher purity, higher average molecular weight and polydispersity, higher content of aliphatic hydroxyl groups, more condensed substructures and less carboxylic groups than hardwood kraft lignins (HKL25 and HKL50). Microscopic observations of CLPs revealed different appearance and morphology in terms of shape, size, inner structures, and surface roughness of produced particles. Moreover, based on the botanical origin of the lignin, clear differences in the surface chemistry of colloidal particles were noticed in the ^{1}HNMR analysis. An opposite behavior against DPPH radical was observed after particle size reduction of kraft lignins based on their botanical origin. It is challenging to compare the results from this study with previously reported ones, due to the differences in the lignin origin, CLPs production process conditions, and resulting physico-chemical characteristics as well as different cellular systems studied. However, we can conclude that CLPs, in general presented higher toxicity than irregular kraft lignin powders towards lung fibroblast cells. Furthermore, in both forms (powder and nanoparticles), softwood kraft lignin showed lower cytotoxic effect than hardwood kraft lignins. Additionally, the toxicity of kraft lignins and corresponding CLPs was dose-dependent; therefore, determined concentrations of these materials that are not toxic for cell systems might be used as an active ingredient in the cosmetic and pharmaceutical sectors.

Table 4
Cell viability (%) of lung fibroblast cell line at different concentrations of lignin and CLPs at 24 h and IC_{30}.

	Cell viability (%)			IC_{30} (μg/mL)
	100 μg/mL	50 μg/mL	25 μg/mL	
SKL	86.2 ± 7.9*	88.4 ± 5.8	88.9 ± 12.0	>100*
HKL25	58.5 ± 8.7*	84.2 ± 6.6	101.6 ± 2.1	77.6*
HKL50	19.4 ± 0.9*	76.9 ± 10.0	89.7 ± 6.3	56.0*
SKL NPs	65.0 ± 4.7*	93.1 ± 6.9*	98.9 ± 0.2	91.1*
HKL25 NPs	48.3 ± 5.8	84.1 ± 8.1	101.3 ± 6.2	69.6
HKL50 NPs	53.2 ± 9.7	78.7 ± 6.7	91.5 ± 7.3	67.1

Data represents mean and standard error from three independent measurements. The population means are significantly different at the 0.05 level according to a one-way analysis of variance (ANOVA).

* The difference between the means is significant at the 0.05 level when comparing cell viability of lignin and colloidal lignin particles (CLPs), according to Bonferroni and Tukey tests.

CRediT authorship contribution statement

Oihana Gordobil: Conceptualization, Methodology, Investigation, Formal analysis, Visualization, Writing – original draft, Funding acquisition. **Huisi Li:** Investigation, Writing – review & editing. **Ana Ayerdi Izquierdo:** Investigation, Methodology, Formal analysis, Validation, Writing – review & editing. **Ainhoa Egizabal:** Writing – review & editing. **Olena Sevastyanova:** Conceptualization, Methodology, Validation, Resources, Writing – review & editing. **Anna Sandak:** Writing – review & editing.

Declaration of competing interest

The authors declare the following financial interests/personal relationships which may be considered as potential competing interests: This research was funded by the European Commission's funding of the InnoRenew project (Grant Agreement #739574 under the Horizon 2020 WIDESPREAD-2-Teaming program) and the Republic of Slovenia (investment funding from the Republic of Slovenia and the European Regional Development Fund). Oihana Gordobil reports financial support was provided by EU Framework Programme for Research and Innovation Marie Sklodowska-Curie Actions. Olena Sevastyanova reports financial support was provided by Knut and Alice Wallenberg Foundation. Huisi Li reports financial support was provided by China Scholarship Council and Wood and Pulping Chemistry Research Network (WPCRN).

Acknowledgements

This research was funded by the European Commission's funding of the InnoRenew project (Grant Agreement #739574 under the Horizon 2020 WIDESPREAD-2-Teaming program) and the Republic of Slovenia (investment funding from the Republic of Slovenia and the European Regional Development Fund). O.G. is grateful for the financial support received from the European Union's Horizon 2020 research and innovation program under the Marie Skłodowska-Curie Action for development of the BIO4CARE project (Grant Number #101023389). The contribution of COST Action LignoCOST (CA17128), supported by COST (European Cooperation in Science and Technology, www.cost.eu), in promoting interaction, exchange of knowledge and collaboration in the field of lignin valorisation is gratefully acknowledged. O.S. is grateful to the Knut and Alice Wallenberg Foundation for financial support through the Wallenberg Wood Science Center at KTH Royal Institute of Technology. H.L. acknowledges The China Scholarship Council and Wood and Pulping Chemistry Research Network (WPCRN) at KTH for the financial support of her doctorate study.

Appendix A. Supplementary data

Supplementary data to this article can be found online at https://doi.org/10.1016/j.ijbiomac.2022.09.111.

References

[1] I.F. Demuner, J.L. Colodette, A.J. Demuner, C.M. Jardim, Biorefinery review: wide-reaching products through kraft lignin, Bioresources 14 (2019) 7543–7581, https://doi.org/10.15376/biores.l4.3.Deuiiuier.

[2] S. Iravani, R.S. Varma, Greener synthesis of lignin nanoparticles and their applications, Green Chem. (2020), https://doi.org/10.1039/c9gc02835h.

[3] Q. Tang, Y. Qian, D. Yang, X. Qiu, Y. Qin, M. Zhou, Lignin-based nanoparticles: a review on their preparations and applications, Polymers 12 (2020) 1–22, https://doi.org/10.3390/POLYM12112471 (Basel).

[4] I.V. Pylypchuk, A. Riazanova, M.E. Lindström, O. Sevastyanova, Structural and molecular-weight-dependency in the formation of lignin nanoparticles from fractionated soft- and hardwood lignins, Green Chem. 23 (2021) 3061–3072, https://doi.org/10.1039/D0GC04058D.

[5] P.S. Chauhan, Lignin nanoparticles: eco-friendly and versatile tool for new era, Bioresour. Technol. Rep. 9 (2020), 100374, https://doi.org/10.1016/j.biteb.2019.100374.

[6] M. Österberg, M.H. Sipponen, B.D. Mattos, O.J. Rojas, Spherical lignin particles: a review on their sustainability and applications, Green Chem. 2712–2733 (2020).

[7] L.E. Low, K.C. Teh, S.P. Siva, I.M.L. Chew, W.W. Mwangi, C.L. Chew, B.H. Goh, E. S. Chan, B.T. Tey, Lignin nanoparticles: the next green nanoreinforcer with wide opportunity, Environ. Nanotechnol.Monit. Manag. 15 (2021), 100398, https://doi.org/10.1016/J.ENMM.2020.100398.

[8] F. Zikeli, M. Romagnoli, G.S. Mugnozza, Lignin nanoparticles in coatings for wood preservation, in: Micro Nanolignin Aqueous Dispersions PolymInteract. Prop. Appl, 2021, pp. 357–384, https://doi.org/10.1016/B978-0-12-823702-1.00014-1.

[9] Y. Qian, X. Zhong, Y. Li, X. Qiu, Fabrication of uniform lignin colloidal spheres for developing natural broad-spectrum sunscreens with high sun protection factor, Ind. Crop. Prod. 101 (2017) 54–60, https://doi.org/10.1016/j.indcrop.2017.03.001.

[10] M. Ago, S. Huan, M. Borghei, J. Raula, E.I. Kauppinen, O.J. Rojas, High-throughput synthesis of lignin particles (~30 nm to ~2 μm) via aerosol flow reactor: size fractionation and utilization in Pickering emulsions, ACS Appl. Mater. Interfaces 8 (2016) 23302–23310, https://doi.org/10.1021/acsami.6b07900.

[11] D.Del Buono, F. Luzi, D. Puglia, Lignin nanoparticles: a promising tool to improve maize physiological, biochemical, and chemical traits, Nanomaterials 11 (2021), https://doi.org/10.3390/NANO11040846 (Basel, Switzerland).

[12] A. do E.S. Pereira, J.Luiz de Oliveira, S.Maira Savassa, C.Barbara Rogério, G. Araujo de Medeiros, L.F. Fraceto, Lignin nanoparticles: new insights for a sustainable agriculture, J. Clean. Prod. 345 (2022), 131145, https://doi.org/10.1016/J.JCLEPRO.2022.131145.

[13] M.H. Sipponen, H. Lange, C. Crestini, A. Henn, M. Österberg, Lignin for nano- and microscaled carrier systems: applications, trends, and challenges, ChemSusChem. 12 (2019) 2039–2054, https://doi.org/10.1002/CSSC.201900480.

[14] M. Witzler, A. Alzagameem, M. Bergs, B. El Khaldi-Hansen, S.E. Klein, D. Hielscher, B. Kamm, J. Kreyenschmidt, E. Tobiasch, M. Schulze, Lignin-derived biomaterials for drug release and tissue engineering, Molecules 23 (2018), https://doi.org/10.3390/MOLECULES23081885.

[15] I.V. Pylypchuk, H. Suo, C. Chucheepchuenkamol, N. Jedicke, P.A. Lindén, M. E. Lindström, M.P. Manns, O. Sevastyanova, T. Yevsa, High-molecular-weight fractions of spruce and eucalyptus lignin as a perspective nanoparticle-based platform for a therapy delivery in liver cancer, Front. Bioeng. Biotechnol. 9 (2022) 1467, https://doi.org/10.3389/FBIOE.2021.817768/BIBTEX.

[16] W. Pei, J. Deng, P. Wang, X. Wang, L. Zheng, Y. Zhang, C. Huang, Sustainable lignin and lignin-derived compounds as potential therapeutic agents for degenerative orthopaedic diseases: a systemic review, Int. J. Biol. Macromol. 212 (2022) 547–560, https://doi.org/10.1016/J.IJBIOMAC.2022.05.152.

[17] Z.S. Chen, M. Yan, W. Pei, B. Yan, C. Huang, H.Y.E. Chan, Lignin-carbohydrate complexes suppress SCA3 neurodegeneration via upregulating proteasomal activities, Int. J. Biol. Macromol. 218 (2022) 690–705, https://doi.org/10.1016/J.IJBIOMAC.2022.07.133.

[18] A. Moreno, J. Liu, M. Morsali, M.H. Sipponen, Chemical modification and functionalization of lignin nanoparticles, in: Micro Nanolignin Aqueous Dispersions Polym. Interact. Prop. Appl, 2022, pp. 385–431, https://doi.org/10.1016/B978-0-12-823702-1.00003-7.

[19] Y. Liu, S. Zhu, Z. Gu, C. Chen, Y. Zhao, Toxicity of manufactured nanomaterials, Particuology 69 (2022) 31–48, https://doi.org/10.1016/J.PARTIC.2021.11.007.

[20] O. Gordobil, R. Herrera, F. Poohphajai, J. Sandak, A. Sandak, Impact of drying process on kraft lignin: lignin-water interaction mechanism study by 2D NIR correlation spectroscopy, J. Mater. Res. Technol. 12 (2021) 159–169, https://doi.org/10.1016/J.JMRT.2021.02.080.

[21] A. Tagami, C. Gioia, M. Lauberts, T. Budnyak, R. Moriana, M.E. Lindström, O. Sevastyanova, Solvent fractionation of softwood and hardwood kraft lignins for more efficient uses: compositional, structural, thermal, antioxidant and adsorption properties, Ind. Crop. Prod. 129 (2019) 123–134, https://doi.org/10.1016/J.INDCROP.2018.11.067.

[22] C.G. Boeriu, D. Bravo, R.J.A. Gosselink, J.E.G. Van Dam, Characterisation of structure-dependent functional properties of lignin with infrared spectroscopy, Ind. Crop. Prod. 20 (2004) 205–218, https://doi.org/10.1016/j.indcrop.2004.04.022.

[23] J. Sameni S. Krigstin M. Sain, Characterization of Lignins Isolated from Industrial Residues and their Beneficial Uses, (n.d.).

[24] A. Granata, D.S. Argyropoulos, 2-Chloro-4,4,5,5-tetramethyl-1,3,2-dioxaphospholane, a reagent for the accurate determination of the uncondensed and condensed phenolic moieties in lignins, J. Agric. Food Chem. 43 (1995) 1538–1544, https://doi.org/10.1021/jf00054a023.

[25] I.V. Pylypchuk, P.A. Lindén, M.E. Lindström, O. Sevastyanova, New insight into the surface structure of lignin nanoparticles revealed by 1H liquid-state NMR spectroscopy, ACS Sustain. Chem. Eng. 8 (2020) 13805–13812, https://doi.org/10.1021/ACSSUSCHEMENG.0C05119/SUPPL_FILE/SC0C05119_SI_001.PDF.

[26] W. Brand-Williams, M.E. Cuvelier, C. Berset, Use of a free radical method to evaluate antioxidant activity, LWTFood Sci. Technol. 28 (1995) 25–30, https://doi.org/10.1016/S0023-6438(95)80008-5.

[27] O. Gordobil, R. Moriana, L. Zhang, J. Labidi, O. Sevastyanova, Assesment of technical lignins for uses in biofuels and biomaterials: structure-related properties, proximate analysis and chemical modification, Ind. Crop. Prod. 83 (2016) 155–165, https://doi.org/10.1016/j.indcrop.2015.12.048.

[28] O. Gordobil, R. Delucis, I. Egüés, J. Labidi, Kraft lignin as filler in PLA to improve ductility and thermal properties, Ind. Crop. Prod. 72 (2015) 46–53, https://doi.org/10.1016/j.indcrop.2015.01.055.

[29] X.F. Zhou, X.J. Lu, Structural characterization of kraft lignin for its green utilization, Wood Res. 59 (2014) 583–592.

[30] O. Sevastyanova, J. Li, G. Geilerstedt, On the reaction mechanism of the thermal yellowing of bleached chemical pulps, Nord. Pulp Pap. Res. J. 21 (2006) 188–192, https://doi.org/10.3183/NPPRJ-2006-21-02-P188-192/MACHINEREADABLECITATION/RIS.

[31] P. Schlee, O. Hosseinaei, C.A. O'Keefe, M. María, J. José, J. Mostazo-López, D. Cazorla-Amorós, A. Amorós, S. Herou, P. Tomani, C.P. Grey, M.-M. Titirici, Hardwood versus softwood Kraft lignin-precursor-product relationships in the manufacture of porous carbon nanofibers for supercapacitors †, 2020, https://doi.org/10.1039/d0ta09093j.

[32] Y.L. Chung, J.V. Olsson, R.J. Li, C.W. Frank, R.M. Waymouth, S.L. Billington, E. S. Sattely, A renewable lignin-lactide copolymer and application in biobased composites, ACS Sustain. Chem. Eng. 1 (2013) 1231–1238, https://doi.org/10.1021/sc4000835.

[33] J. Zhao, W. Xiuwen, J. Hu, Q. Liu, D. Shen, R. Xiao, Thermal degradation of softwood lignin and hardwood lignin by TG-FTIR and Py-GC/MS, Polym. Degrad. Stab. 108 (2014) 133–138, https://doi.org/10.1016/j.polymdegradstab.2014.06.006.

[34] M. Balakshin, E. Capanema, On the quantification of lignin hydroxyl groups with 31P and 13C NMR spectroscopy, J. Wood Chem. Technol. 35 (2015) 220–237, https://doi.org/10.1080/02773813.2014.928328.

[35] S. Constant, H.L.J. Wienk, A.E. Frissen, P. de Peinder, R. Boelens, D.S. van Es, R.J. H. Grisel, B.M. Weckhuysen, W.J.J. Huijgen, R.J.A. Gosselink, P.C.A. Bruijnincx, New insights into the structure and composition of technical lignins: a comparative characterisation study, Green Chem. 18 (2016) 2651–2665, https://doi.org/10.1039/C5GC03043A.

[36] X. Wei, Y. Liu, Y. Luo, Z. Shen, S. Wang, M. Li, L. Zhang, Effect of organosolv extraction on the structure and antioxidant activity of eucalyptus kraft lignin, Int. J. Biol. Macromol. 187 (2021) 462–470, https://doi.org/10.1016/J.IJBIOMAC.2021.07.082.

[37] H. Zhang, Y. Bai, B. Yu, X. Liu, F. Chen, A practicable process for lignin color reduction: fractionation of lignin using methanol/water as a solvent, Green Chem. 19 (2017) 5152–5162, https://doi.org/10.1039/c7gc01974b.

[38] H. Li, Y. Deng, J. Liang, Y. Dai, B. Liu, Y. Ren, X. Qiu, C. Li, Hollow lignin nanospheres, Bioresources 11 (2016) 3073–3083.

[39] J.L. Wen, S.L. Sun, B.L. Xue, R.C. Sun, Recent advances in characterization of lignin polymer by solution-state nuclear magnetic resonance (NMR) methodology, Materials 6 (2013) 359–391, https://doi.org/10.3390/ma6010359 (Basel).

[40] S. Constant, H.L.J. Wienk, A.E. Frissen, P. De Peinder, R. Boelens, D.S. Van Es, R.J. H. Grisel, B.M. Weckhuysen, W.J.J. Huijgen, R.J.A. Gosselink, P.C.A. Bruijnincx, New insights into the structure and composition of technical lignins: a comparative characterisation study, Green Chem. 18 (2016) 2651–2665, https://doi.org/10.1039/C5GC03043A.

[41] S.N. Sun, M.F. Li, T.Q. Yuan, F. Xu, R.C. Sun, Sequential extractions and structural characterization of lignin with ethanol and alkali from bamboo (Neosinocalamus affinis), Ind. Crop. Prod. 37 (2012) 51–60, https://doi.org/10.1016/j.indcrop.2011.11.033.

[42] M.H. Sipponen, H. Lange, M. Ago, C. Crestini, Understanding lignin aggregation processes. A case study: budesonide entrapment and stimuli controlled release from lignin nanoparticles, ACS Sustain.Chem. Eng. 6 (2018) 9342–9351, https://doi.org/10.1021/ACSSUSCHEMENG.8B01652.

[43] K. Lundquist, 1H NMR spectral studies of lignins, Nord. Pulp Pap. Res. J. 1 (1992) 4–16.

[44] E. Sjöström, Lignin, Wood Chem. (1993) 71–89, https://doi.org/10.1016/B978-0-08-092589-9.50008-5.

[45] W.O.S. Doherty, P. Mousavioun, C.M. Fellows, Value-adding to cellulosic ethanol: lignin polymers, Ind. Crop. Prod. 33 (2011) 259–276, https://doi.org/10.1016/j.indcrop.2010.10.022.

[46] O. Gordobil, R. Moriana, L. Zhang, J. Labidi, O. Sevastyanova, Assesment of technical lignins for uses in biofuels and biomaterials: structure-related properties, proximate analysis and chemical modification, Ind. Crop. Prod. 83 (2016), https://doi.org/10.1016/j.indcrop.2015.12.048.

[47] O. Gordobil, R. Delucis, I. Egüés, J. Labidi, Kraft lignin as filler in PLA to improve ductility and thermal properties, Ind. Crop. Prod. 72 (2015), https://doi.org/10.1016/j.indcrop.2015.01.055.

[48] K. Lundquist, Proton (1H) NMR spectroscopy, in: S.Y. Lin, C.W. Dence (Eds.), Methods Lignin Chem, Springer Berlin Heidelberg, Berlin, Heidelberg, 1992, https://doi.org/10.1007/978-3-642-74065-7.
[49] M.A. Jedrzejczyk, S. Van Den Bosch, V. Aelst, K. Van Aelst, P.D. Kouris, M. Moalin, G.R.M.M. Haenen, M.D. Boot, E.J.M. Hensen, B. Lagrain, B.F. Sels, K.V. Bernaerts, Lignin-based additives for improved thermo-oxidative stability of biolubricants, 2021, https://doi.org/10.1021/acssuschemeng.1c02799.
[50] D. Piccinino, E. Capecchi, E. Tomaino, S. Gabellone, V. Gigli, D. Avitabile, R. Saladino, Nano-structured lignin as green antioxidant and UV shielding ingredient for sunscreen applications, Antioxidants 10 (2021) 274, https://doi.org/10.3390/ANTIOX10020274.
[51] V. Ugartondo, M. Mitjans, M.P. Vinardell, Comparative antioxidant and cytotoxic effects of lignins from different sources, Bioresour. Technol. 99 (2008) 6683–6687, https://doi.org/10.1016/j.biortech.2007.11.038.
[52] W. Yang, E. Fortunati, D. Gao, G.M. Balestra, G. Giovanale, X. He, L. Torre, J. M. Kenny, D. Puglia, Valorization of acid isolated high yield lignin nanoparticles as innovative antioxidant/antimicrobial organic materials, ACS Sustain. Chem. Eng. 6 (2018) 3502–3514, https://doi.org/10.1021/acssuschemeng.7b03782.
[53] T. Dizhbite, G. Telysheva, V. Jurkjane, U. Viesturs, Characterization of the radical scavenging activity of lignins - natural antioxidants, Bioresour. Technol. 95 (2004) 309–317, https://doi.org/10.1016/j.biortech.2004.02.024.
[54] J. Ponomarenko, T. Dizhbite, M. Lauberts, A. Volperts, G. Dobele, G. Telysheva, Analytical pyrolysis - a tool for revealing of lignin structure-antioxidant activity relationship, J. Anal. Appl. Pyrolysis 113 (2015) 360–369, https://doi.org/10.1016/j.jaap.2015.02.027.
[55] M. Lauberts, O. Sevastyanova, J. Ponomarenko, T. Dizhbite, G. Dobele, A. Volperts, L. Lauberte, G. Telysheva, Fractionation of technical lignin with ionic liquids as a method for improving purity and antioxidant activity, Ind. Crop. Prod. 95 (2017) 512–520, https://doi.org/10.1016/j.indcrop.2016.11.004.
[56] S. Aminzadeh, M. Lauberts, G. Dobele, J. Ponomarenko, T. Mattsson, M. E. Lindström, O. Sevastyanova, Membrane filtration of kraft lignin: structural charactristics and antioxidant activity of the low-molecular-weight fraction, Ind. Crop. Prod. 112 (2018) 200–209, https://doi.org/10.1016/J.INDCROP.2017.11.042.
[57] Q. Lu, M. Zhu, Y. Zu, W. Liu, L. Yang, Y. Zhang, X. Zhao, X. Zhang, X. Zhang, W. Li, Comparative antioxidant activity of nanoscale lignin prepared by a supercritical antisolvent (SAS) process with non-nanoscale lignin, Food Chem. 135 (2012) 63–67, https://doi.org/10.1016/J.FOODCHEM.2012.04.070.
[58] M.R.V. Bertolo, L.B. Brenelli de Paiva, V.M. Nascimento, C.A. Gandin, M.O. Neto, C.E. Driemeier, S.C. Rabelo, Lignins from sugarcane bagasse: renewable source of nanoparticles as Pickering emulsions stabilizers for bioactive compounds encapsulation, Ind. Crop. Prod. 140 (2019), 111591, https://doi.org/10.1016/J.INDCROP.2019.111591.
[59] S.R. Yearla, K. Padmasree, Preparation and characterisation of lignin nanoparticles: evaluation of their potential as antioxidants and UV protectants, J. Exp. Nanosci. 11 (2016) 289–302, https://doi.org/10.1080/17458080.2015.1055842.
[60] N. Giummarella, P.A. Lindén, D. Areskogh, M. Lawoko, Fractional profiling of kraft lignin structure: unravelling insights on lignin reaction mechanisms, ACS Sustain. Chem. Eng. 8 (2020) 1112–1120, https://doi.org/10.1021/ACSSUSCHEMENG.9B06027/SUPPL_FILE/SC9B06027_SI_001.PDF.
[61] L. Zheng, G. Lu, W. Pei, W. Yan, Y. Li, L. Zhang, C. Huang, Q. Jiang, Understanding the relationship between the structural properties of lignin and their biological activities, Int. J. Biol. Macromol. 190 (2021) 291–300, https://doi.org/10.1016/J.IJBIOMAC.2021.08.168.
[62] G. Bystrzejewska-Piotrowska, J. Golimowski, P.L. Urban, Nanoparticles: their potential toxicity, waste and environmental management, Waste Manag. 29 (2009) 2587–2595, https://doi.org/10.1016/j.wasman.2009.04.001.
[63] G.J. Gil-Chávez, S.S.P. Padhi, C.V. Pereira, J.N. Guerreiro, A.A. Matias, I. Smirnova, Cytotoxicity and biological capacity of sulfur-free lignins obtained in novel biorefining process, Int. J. Biol. Macromol. 136 (2019) 697–703, https://doi.org/10.1016/j.ijbiomac.2019.06.021.
[64] M.P. Vinardell, V. Ugartondo, M. Mitjans, Potential applications of antioxidant lignins from different sources, Ind. Crop. Prod. 27 (2008) 220–223, https://doi.org/10.1016/j.indcrop.2007.07.011.
[65] F.M.C. Freitas, M.A. Cerqueira, C. Gonçalves, S. Azinheiro, A. Garrido-Maestu, A. A. Vicente, L.M. Pastrana, J.A. Teixeira, M. Michelin, Green synthesis of lignin nano- and micro-particles: physicochemical characterization, bioactive properties and cytotoxicity assessment, Int. J. Biol. Macromol. 163 (2020) 1798–1809, https://doi.org/10.1016/j.ijbiomac.2020.09.110.
[66] P. Figueiredo, K. Lintinen, A. Kiriazis, V. Hynninen, Z. Liu, T. Bauleth-Ramos, A. Rahikkala, A. Correia, T. Kohout, B. Sarmento, J. Yli-Kauhaluoma, J. Hirvonen, O. Ikkala, M.A. Kostiainen, H.A. Santos, In vitro evaluation of biodegradable lignin-based nanoparticles for drug delivery and enhanced antiproliferation effect in cancer cells, Biomaterials 121 (2017) 97–108, https://doi.org/10.1016/j.biomaterials.2016.12.034.